



HAL
open science

Planar microlenses for near infrared CMOS image sensors

L. Dilhan, Jérôme Vaillant, A. Ostrovsky, L. Masarotto, C. Pichard, R. Paquet

► **To cite this version:**

L. Dilhan, Jérôme Vaillant, A. Ostrovsky, L. Masarotto, C. Pichard, et al.. Planar microlenses for near infrared CMOS image sensors. *Electronic Imaging*, 2020, 32 (7), pp.144-1-144-7. 10.2352/ISSN.2470-1173.2020.7.ISS-144 . hal-04235049

HAL Id: hal-04235049

<https://hal.science/hal-04235049>

Submitted on 10 Oct 2023

HAL is a multi-disciplinary open access archive for the deposit and dissemination of scientific research documents, whether they are published or not. The documents may come from teaching and research institutions in France or abroad, or from public or private research centers.

L'archive ouverte pluridisciplinaire **HAL**, est destinée au dépôt et à la diffusion de documents scientifiques de niveau recherche, publiés ou non, émanant des établissements d'enseignement et de recherche français ou étrangers, des laboratoires publics ou privés.

Planar microlenses for near infrared CMOS image sensors

L. Dilhan^{1,2}, J. Vaillant², A. Ostrovsky¹, L. Masarotto², C. Pichard², R. Paquet²;

¹STMicroelectronics; 850 rue Jean Monnet, F-38920 Crolles; France

²Univ. Grenoble Alpes, CEA, LETI; F38000 Grenoble, France

Abstract

In this paper we present planar microlenses designed to improve the sensitivity of SPAD pixels. We designed diffractive and metasurface planar microlens structures based on rigorous optical simulations, then we implemented the diffractive microlens on a SPAD design available on STMicroelectronics 40nm CMOS testchips (32×32 SPAD array), and compared with the process of reference melted microlens. We characterized circuits and demonstrated optical gain from our designed microlenses (numbers to be added).

Introduction

Our work centers on designing a wafer level planar microlens for applications in near-infrared, on Single Photon Avalanche Diode (SPAD). The current solution, which is the melted microlens [1], and two new types of planar microlenses will be compared to a SPAD without microlens to assess gain of the different microlenses. Rigorous optical simulations are performed using a FDTD-solutions software [2].

SPAD macropixel

Single photon avalanche diode arrays are used in applications requiring photon counting over time, with accuracy around hundreds of picoseconds or less. The applications are set with active illumination with monochromatic wavelength of either 850, 905 or 940 nm, the latter being the most critical, being the least absorbed wavelength by the photo-sensitive area of the pixel.

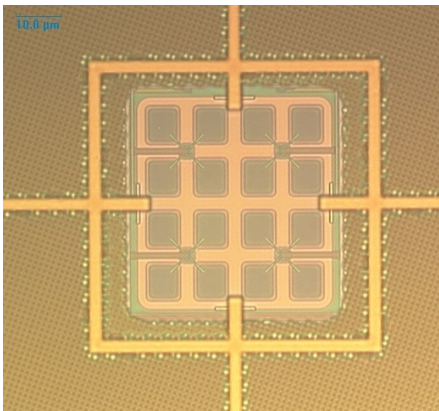


Figure 1: SPAD macropixel layout

One SPAD layout is considered in this work, on Front-Side Illumination (FSI) STMicroelectronics 40 nm CMOS technology, with a $11 \mu\text{m}$ pixel pitch [3]. The macropixels, see Fig. 1, are designed to share the diode N-well between 4×4 SPAD, allowing the pixels to have a fill-factor of $\sim 40\%$ [4]. Light entering the upper layer of a SPAD pixel has to go through $5.4 \mu\text{m}$ of Back-

End of Line stack thickness before reaching the photo-sensitive area, and encounters metal layers on its path, such being reflected and scattered in all directions before reaching the silicon layer.

Current process: melted microlens

We want to design a microlens that focuses the light inside the SPAD pixel, to avoid the metal layers in the stack and enhance the fill-factor. This microlens is deposited by photo-lithography, then melted to reach the desired dome-shape [5].

Given the symmetry of the macropixel, see Fig. 1, we simulate only a quarter of the macropixel. Fig. 2 represents a vertical cross section of a quarter of macropixel simulated, with the melted microlens. The colorbar indicates the index of refraction of the medium. The red bottom layer is the Silicon (Si), containing the photo-sensitive part of the pixel thus where we want to concentrate light, and the dark blue top layer is the entry medium, air. The melted microlens has a thickness of $4 \mu\text{m}$ over the pixel, with a varying topography along the x and y axis.

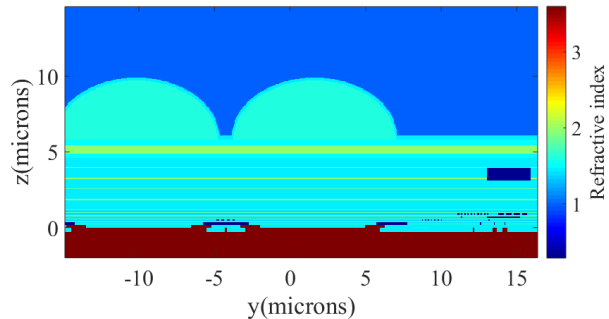


Figure 2: 2 SPAD pixels index cross-section, with melted microlens implemented

Towards planar microlenses

A planar microlens has the advantage of being processed with common lithography-etch steps, with a shape defined by design and not through process adjustments, allowing dedicated design per pixel.

We start by investigating a diffractive planar solution, commonly referred to as Fresnel Zone Plate (FZP) microlens, conventionally used as a concentrative X-ray lens [6] [7] but also on SPAD arrays [8] [9]. Then we explore the metasurfaces [10], finding a way to apply them to our application.

We present the theory behind each planar microlens, then the simulation results and finally the characterization results for all but metasurface microlenses.

Theory

We use two approaches to find a good suited planar microlens. Firstly, we consider the known FZP microlens [7] [8] and adapt it to our needs. Secondly, we investigate the use of a metasurface as a microlens [11].

FZP microlens

The FZP microlens is based on the principle of diffraction, designed to focus light by constructive interferences in focus spots determined by the geometry of the microlens. The intensity is highest in the first order of diffraction, and other orders are negligible. In Fig. 3, a theoretical FZP principle schematic, we see the entry material, serving as an anti-reflective (AR) coating, with a refractive index n_{AR} , encapsulating the FZP microlens, with index n_{FZP} here. The FZP lens lies on an output material of index n .

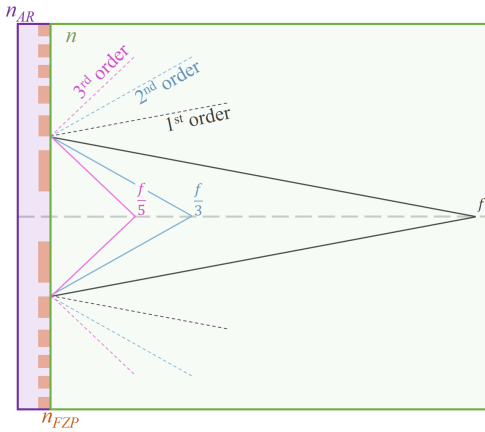


Figure 3: FZP lens diffraction principle

The conventional FZP lens is composed of concentric diffracting rings, with given inner and outer radii for each ring. The k -th radius of the rings is defined as follows:

$$r_k = \sqrt{\frac{k\lambda}{n} \left(f + \frac{k\lambda}{4n} \right)} \quad (1)$$

Where k the radius number, f the focal length of the FZP microlens, λ the working wavelength and n the index of refraction of the output material, a design of FZP microlens resulting from equation 1 is shown in Fig. 4.

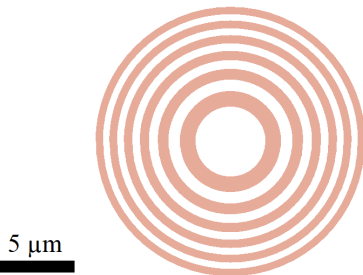


Figure 4: FZP microlens example design

In a regular amplitude FZP lens the diffracting material is an absorbant material, often metal. Here, we want to maximise the transmission of the FZP microlens, thus we design a phase FZP, where the material is chosen to specifically introduce a π phase shift between the zones with different materials. We control the

phase shift by controlling the material's thickness h . In our study, we chose amorphous silicon (a:Si) as the phase-shifting material, and silicon oxide as an anti-reflective coating, to have a high refractive index contrast. The thickness h is given by:

$$h = \frac{(2m+1)\lambda}{2(n_{a:Si} - n_{AR})} \quad (2)$$

Here m is an integer giving the different thicknesses for which the interferences are constructive between the light going through the high index material and the light going through the AR material. $n_{a:Si}$ is the refractive index of a:Si and n_{AR} is the refractive index of the other material, anti-reflective coating or air. m is chosen by considering process capability, here we used the thinnest solution ($m = 0$).

Metasurface

Nanopillars of high refractive index with dimensions largely inferior to the working wavelength can be designed to be phase shifters [10]. We create a library of nanopillars by simulating nanopillars with infinite periodic boundaries with given height, radius, material and pitch. Each simulation yields a result of phase shift for a particular set of parameters. We then use the information to set our desired array of nanopillars to form a metasurface, assuming that the nanopillars yield the same phase in a periodic array of similar pillars than surrounded by nanopillars with different set of parameters. It is necessary, when constructing the library, to create a set of nanopillars covering a 2π phase shift. In our case, we design a metasurface (array of nanopillars) so that the light is focused at a desired focal length, creating a metamicro-lens. We use equation 3 to describe the phase-shift ϕ induced by an infinite plano-convex perfect lens, with a given focal length f [11].

$$\phi(r) = \left[\frac{2\pi}{\lambda} \left(\sqrt{r^2 + f^2} - f \right) \right] \text{mod}(2\pi) \quad (3)$$

We match the nanopillars from the library to the dashed line of the phase profile shown in Fig. 5, thus designing a metamicro-lens. When choosing the nanopillars from the library, we select them to have the highest possible transmission, in order to lose as little signal as possible.

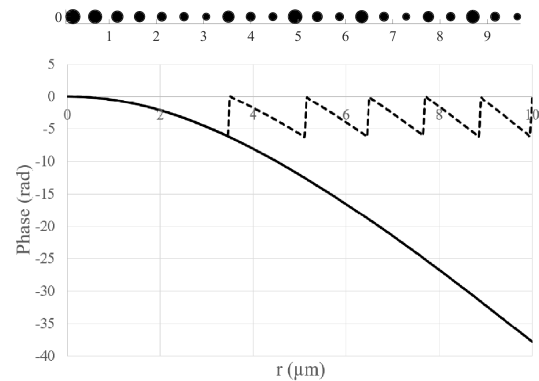


Figure 5: Infinite plano-convex lens phase profile given by eq. 3, with and without the 2π modulus, with corresponding phase pillars

In Fig. 5 is represented the nanopillars selected from the library to match the phase profile shown in below Fig. 5. The whole metamicro-lens is formed with different nanopillars, and then simulated rigorously.

Simulations

In this part, we simulate the propagation of light [12] through the microlens into the pixels, and compare it to the reference, the pixel without microlens. In our study, we work with a plane wave with $\lambda = 940 \pm 5$ nm, and with all simulations we use the same 2×2 SPAD design and parameters, changing only the microlens from one simulation to the other. Our metrics are the absorption in the depleted region of the pixel, and the optical gain comparing the absorption without and with microlens.

No microlens, reference

Knowing the architecture of a 4×4 SPAD design, a reference simulation is done without microlens.

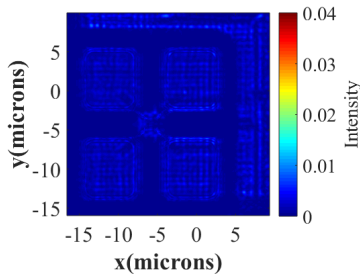


Figure 6: Light intensity at photo-sensitive area entry, no microlens

Fig. 6 represents the light intensity at the plane of entry of the photo-sensitive area. We see the imprint of the metal layers in the intensity distribution, and see that light is lost over areas where there is no photo-sensitive areas. This is explained by the fact that light is going through several metal layers before reaching the photo-sensitive area, thus being scattered on its path.

Melted microlens

We make a 3D FIB-SEM characterization of the surface of a melted microlens produced at STMicroelectronics, and simulate it in the software, to have a simulation as close to reality as possible.

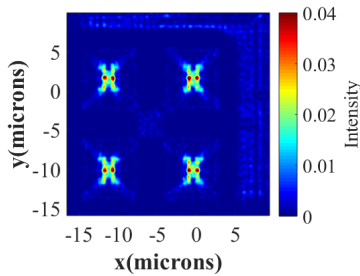


Figure 7: Light intensity at photo-sensitive area entry, melted microlens

Comparing Fig. 7 to Fig. 6, we see that here the light is focused in the photo-sensitive area, and thus the absorption in them is increased. Here the gain is 1.6.

FZP microlens

Here, we put the FZP microlens on an output material of index $n = 1.45$, see equation 1. We use a:Si as the high-refractive index, and SiO₂ as the anti-reflective coating. We put a pedestal of a few μm to allow some supplementary converging distance for the incoming light, thus avoiding the metal layers. The variables of the simulations are the focal length f , the pedestal thickness th and h the thickness of the FZP microlens.

Modifying f has an effect on the radii of the rings and thus the design of the FZP microlens whereas modifying h has an effect on the etching process of fabrication of the FZP microlens.

We optimize those parameters and thus the FZP microlens design, to have the highest possible absorption in the bottom photo-sensitive layer.

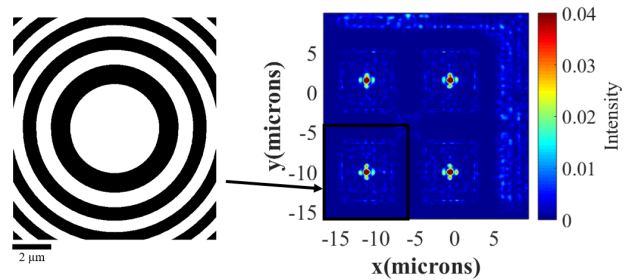


Figure 8: Top view of FZP microlens and light intensity at photo-sensitive area entry simulation result

With our design, we see in Fig. 8 that light is tightly focused at the surface of the photo-sensitive layer. We have a focus-spot with a diameter of $\sim 0.5 \mu\text{m}$ FWHM, with a gain of 1.2 compared to the simulation without microlens.

Metamicro-lens

After building the library of nanopillars composed of high refractive index a:Si nanopillars in SiO₂ medium, we simulate a metamicro-lens with the same focal length as the FZP microlens to have comparable results. We choose a:Si and SiO₂ to have a high index contrast between the two materials and because those two materials can theoretically be processed with our parameters at the STMicroelectronics clean-room.

As with the melted and FZP microlenses, we see that the metamicro-lens focuses light at the photo-sensitive layer's surface.

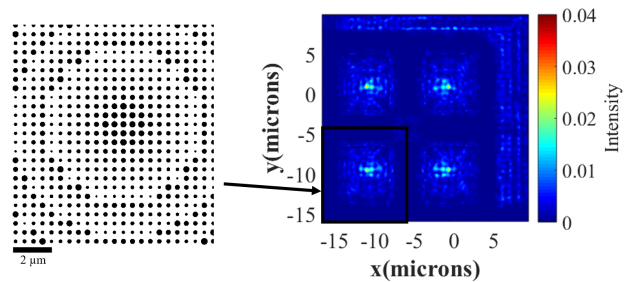


Figure 9: Top view of metamicro-lens and light intensity at photo-sensitive area entry simulation result

With our design, we see a gain of 1.6 compared to the simulation without microlens, which is slightly better than the FZP microlens result, as the $0 - 2\pi$ phase shift is sampled better here.

Simulation results

In table 1 are the absorption and gain in the photo-sensitive area given by the simulations. The absorption is given as the average of the four SPAD pixels simulated's absorption. We expect to find similar results with the characterization measurements performed on the SPAD pixel without microlens, with melted microlens and with FZP microlens. The metasurface process is yet to be developed and thus the metamicrolens has not yet been fabricated.

Table 1: Expected results from simulation

Simulation	Absorption (%)	Gain
No lens	2.10 ± 0.10	–
Melted microlens	3.40 ± 0.09	1.6
FZP microlens	2.56 ± 0.03	1.2
Metamicrolens	2.94 ± 0.04	1.4

These results are promising, as we can see that all the microlenses yield gain. Looking at the expected results for the metamicrolens, we can suppose that its performances will exceed the ones of the FZP microlens, once the process will be developed.

Characterization

In this part, we fabricated and characterized 4×4 SPAD pixels without microlens, with the current solution of melted microlens and with the FZP microlens. On Fig. 10 are shown top views of the melted and FZP microlens, left and right respectively, after fabrication.

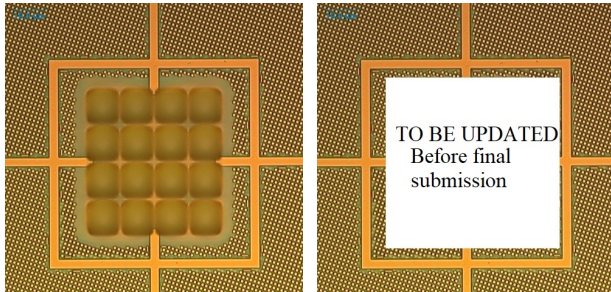


Figure 10: Top view of SPAD macropixel with left: melted microlens, right: FZP microlens

We perform photon detection efficiency (PDE) measurements at wafer level, with a uniform narrow bandwidth illumination, with an aperture $f/2$. For each die, mean value and standard deviation over the SPADs are computed. From the PDE of the measured dies, we compute the gain for each microlens, compared to a SPAD without microlens. The characterization measurements led to the results presented in table 2.

Table 2: Characterization results

Simulation	PDE	Gain
No lens	1.2	–
Melted microlens	2.7	2.25
FZP microlens	tbu	tbu

Comparing table 1 and table 2, we can only compare the gain column, to compare relatively the simulations and the characterization, as both are not done with the exact same parameters.

The measurements on wafer without microlens and with a melted microlens has been done, however the measurements on the FZP microlens are ongoing. The results will be updated and added in the final version of the paper.

Conclusion

In this study, we have demonstrated the capability to improve SPAD sensitivity by using different types of microlenses in the near infrared. Considering Fresnel Zone Plate and metasurface structures, we designed microlenses based on rigorous optical simulations taking into account the SPAD layout, the CMOS technology and the current microlens solution. The current microlens solution and Fresnel Zone Plate microlens were implemented on STMicroelectronics 40nm CMOS testchips and gains of 2.25 and tbu in sensitivity respectively were measured compared to a SPAD without microlens. The technologies described in this paper offer several advantages like planarization, simplicity in process and design or the capability to focus light.

References

- [1] G. Intermite et al, Enhancing the Fill-Factor of CMOS SPAD Arrays Using Microlens Integration, Proceedings of SPIE, Vol. 9504 (2015).
- [2] High-Performance Nanophotonic Simulation Software, <http://www.lumerical.com/>.
- [3] S. Pellegrini et al, Industrialised SPAD in 40 Nm Technology, 2017 IEEE International Electron Devices Meeting (IEDM), pp. 16.5.1-16.5.4 (2017).
- [4] S. Pellegrini, International SPAD sensor workshop (2018).
- [5] Y.-T. Fan, C.-S. Peng, et C.-Y. Chu, Advanced microlens and color filter process technology for the high-efficiency CMOS and CCD image sensors, vol. 4115, p. 263-274 (2000).
- [6] A. G. Michette, Optical Systems for Soft X-Rays, Plenum, London (1986).
- [7] Max Born et al, Principles of Optics: Electromagnetic Theory of Propagation, Interference and Diffraction of Light, 7th ed. Cambridge University Press (1999).
- [8] J. Vaillant et al, SPAD array sensitivity improvement by diffractive microlens, International Image Sensor Workshop (IISW), P28 (2019).
- [9] F. Hirigoyen, Fresnel Zone Plates : plasmonics filtering for SPADs sensors, International Image Sensor Workshop (IISW), P45 (2017).
- [10] Lalanne, P., Chavel, P., Laser & Photonics Reviews, 11, 1600295 (2017).
- [11] Yu, N. & Capasso, F., Flat optics with designer metasurfaces, Nature Materials, Nature Publishing Group, a division of Macmillan Publishers Limited. All Rights Reserved., 13, 139 (2014).
- [12] A. Crocherie et al, Three-Dimensional Broadband FDTD Optical Simulations of CMOS Image Sensor, vol. 7100, 71002J-71002J-12 (2008).

Author Biography

Lucie Dilhan received her M. Sc. in Optical Physics from Institut d'Optique Graduate School in Palaiseau, France (2017) and her M. Sc. in Biomedical Physics from the Royal Institute of Technology in Stockholm, Sweden (2018). Since then she is pursuing with a PhD conducted between STMicroelectronics R&D center in Crolles, France, and CEA in Grenoble, France. Her work is focused on the development

of planar microlenses for imager applications.

Jérôme Vaillant received his M. Sc. in Optical Engineering from Ecole Centrale de Marseille, France (1996), his M. Sc. Degree in Astrophysics from Grenoble Alps University, France (1997) and his Ph.D. in Astrophysics from Lyon University, France, in 2000. Since then he has worked on CMOS image sensor with a focus on optics at pixel. Starting in 2000 at STMicroelectronics R&D center in Crolles, France, he joined CEA in Grenoble, France, in 2012.

Alain Ostrovsky received the M. Sc. in Opto-electronics and Micro-electronics from Ecole Nationale Supérieure d'Ingénieurs, Caen ISMRa, in 1994. He joined the Thin film group of Jobin Yvon company in the US for 5 years concentrating on ellipsometry and optical endpoint for micro-electronic industry. He joined STMicroelectronics Crolles in 2000 to develop integrated metrology solutions, since 2008 he works as lithography process engineer developing R&D CMOS digital and CMOS image sensor technologies.

Lilian Masarotto received his M. Sc. in Material Sciences from Institut National des Sciences Appliquées, Toulouse, France (1998) and his Ph.D. in Integrated Electronic devices from Institut National des Sciences Appliquées, Lyon, France, in 2001. In 2002, he joined CEA-Leti in Grenoble and worked on developing high thermal deposition processes of thin layers and nanocrystals by RPCVD or vertical LPCVD tools. Since 2011, he has worked on the development of integrated optical structures on CMOS image sensors.

Céline Pichard received her BTEC National Diploma in Thermal Engineering and Energy from Joseph Fourier University in Grenoble, France (2001). Since then she has worked on production process, starting in 2001 at STMicroelectronics R&D center in Crolles, France, she joined CEA in Grenoble, France, in 2018.

Romain Paquet...